JGP Journal of General Physiology

RESEARCH ARTICLE

Phase 1 repolarization rate defines Ca^{2+} dynamics and contractility on intact mouse hearts

María Micaela López Alarcón[1], Ainhoa Rodríguez de Yurre[1], Juan Ignacio Felice[2], Emiliano Medei[1], and Ariel L. Escobar[3]

In the heart, Ca^{2+} influx through L-type Ca^{2+} channels triggers Ca^{2+} release from the sarcoplasmic reticulum. In most mammals, this influx occurs during the ventricular action potential (AP) plateau phase 2. However, in murine models, the influx through L-type Ca^{2+} channels happens in early repolarizing phase 1. The aim of this work is to assess if changes in the open probability of 4-aminopyridine (4-AP)–sensitive Kv channels defining the outward K^+ current during phase 1 can modulate Ca^{2+} currents, Ca^{2+} transients, and systolic pressure during the cardiac cycle in intact perfused beating hearts. Pulsed local-field fluorescence microscopy and loose-patch photolysis were used to test the hypothesis that a decrease in a transient K^+ current (I_{to}) will enhance Ca^{2+} influx and promote a larger Ca^{2+} transient. Simultaneous recordings of Ca^{2+} transients and APs by pulsed local-field fluorescence microscopy and loose-patch photolysis showed that a reduction in the phase 1 repolarization rate increases the amplitude of Ca^{2+} transients due to an increase in Ca^{2+} influx through L-type Ca^{2+} channels. Moreover, 4-AP induced an increase in the time required for AP to reach 30% repolarization, and the amplitude of Ca^{2+} transients was larger in epicardium than endocardium. On the other hand, the activation of I_{to} with NS5806 resulted in a reduction of Ca^{2+} current amplitude that led to a reduction of the amplitude of Ca^{2+} transients. Finally, the 4-AP effect on AP phase 1 was significantly smaller when the L-type Ca^{2+} current was partially blocked with nifedipine, indicating that the phase 1 rate of repolarization is defined by the competition between an outward K^+ current and an inward Ca^{2+} current.

Introduction

The cardiac ventricular action potential (AP) is the earliest physiological event that controls contraction during the cardiac cycle. Typically, the prolonged duration of the ventricular AP allows an increase in the L-type Ca^{2+} channel open probability, leading to a sustained influx of Ca^{2+} into the myocyte. In small mammals, the duration of the AP needs to be short enough to cope with a higher heart rate. In a mouse, the heart rate can be as high as 600 beats/min, setting the total duration of the AP to values shorter than 100 ms. This fact led researchers to assume that the time course of a mouse ventricular AP lacks a plateau phase (phase 2; Nerbonne and Kass, 2005; Dilly et al., 2006). However, our laboratory recently demonstrated that when APs are recorded in situ at the intact organ level, the mouse ventricular AP displays a phase 2 (Ferreiro et al., 2012; Ramos-Franco et al., 2016). Additionally, we found that this phase 2 was more hyperpolarized than in larger mammals (Kornyeyev et al., 2010; Valverde et al., 2010; Ferreiro et al., 2012) and was driven by an influx of Na^+ through the Na^+-Ca^{2+} exchanger (NCX; Ramos-Franco et al., 2016). Moreover, we demonstrated that in the intact heart, the influx of Ca^{2+} that triggers Ca^{2+} transients occurs during the deactivation of L-type Ca^{2+} channels in AP phase 1 (Ramos-Franco et al., 2016). Although other groups have proposed this idea for different mammalian species such as dog (Zygmunt et al., 1997; Bányász et al., 2003; Cordeiro et al., 2004), rat (Bouchard et al., 1995; Sah et al., 2002; Cooper et al., 2010), and mouse (Dilly et al., 2006; Kondo et al., 2006), those experiments were performed mostly in isolated ventricular myocytes under voltage-clamp conditions. Even though that approach has been extremely helpful, the "exact" ventricular region and layer from which the tested dissociated myocytes originated was not precisely defined. Furthermore, the electric, metabolic, and mechanical coupling between cells at different layers is lost when cells are isolated. Moreover, at the intact heart level there is a transmural electrical gradient that defines the excitation-contraction coupling properties; this electrical gradient is also missing when the myocytes are isolated. Finally, ionic currents in isolated myocytes are usually recorded at room temperature, at bradycardic pacing rates, and in the presence of exogenous intracellular Ca^{2+} buffers to help with cell viability, a condition that also changes the properties of Ca^{2+} dynamics during diastole and systole.

[1]Instituto de Biofísica Carlos Chagas Filho, Universidade Federal do Rio de Janeiro, Brazil; [2]Centro de Investigaciones Cardiovasculares, Universidad Nacional de La Plata, La Plata, Argentina; [3]Department of Bioengineering, School of Engineering, University of California, Merced, CA.

Correspondence to Ariel L. Escobar: aescobar4@ucmerced.edu.

In the present article, we propose to gauge the role of a key K^+ conductance activated during phase 1 repolarization in defining the transmural Ca^{2+} signaling. An integrated and simultaneous assessment of the mechanical activity, AP kinetics, electrocardiograms (ECGs), Ca^{2+} transients, and Ca^{2+} currents was performed on intact perfused hearts when Kv channels were inhibited by 4-aminopyridine (4-AP) or activated with 1-[2,4-dibromo-6-(1H-tetrazol-5-yl)-phenyl]-3-(3,5-bis-trifluoromethyl-phenyl)-urea (NS5806). We think that understanding the kinetics of phase 1 repolarization in different ventricular layers will help us to understand not only transmural electrical repolarization but also mechanical dysfunctions. Furthermore, the knowledge obtained from the experiments presented here will help us understand pathophysiological mechanisms related to systolic heart failure and define novel pharmacological interventions to treat this set of clinical conditions.

Material and methods

Ethical approval

All animal experiments were performed on adult mice (Charles River Laboratories) in accordance with the Institutional Animal Care and Use Committee of the University of California Merced. Animals were maintained by the National Institutes of Health Guide for the Care and Use of Laboratory Animals (National Institutes of Health Publication No. 85-23, Revised 1996). The Institutional Animal Care and Use Committee of the University of California Merced approved the euthanasia method used (#2008–201).

Whole-heart preparation

Hearts were obtained from 8-wk-old Balb/C male mice (Charles River Laboratories). Animals were injected intraperitoneally with Na^+-heparin and euthanized by cervical dislocation 15 min after the injection. The heart was rapidly removed, and the aorta was cannulated onto a standard horizontal (Zimmer, 1998; Mejía-Alvarez et al., 2003) Langendorff apparatus for continuous perfusion with normal Tyrode's solution containing, in mM, NaCl 140, KCl 5.3, $CaCl_2$ 2, $MgCl_2$ 1, $NaPO_4H_2$ 0.33, HEPES 10, and glucose 10. The osmolarity of the solution was 295 mOsm/L, and the pH, 7.4. After spontaneous cardiac contractility became regular, hearts were loaded with either Ca^{2+}-sensitive or voltage-sensitive fluorescent indicators. Specifically, Rhod-2AM or Di-8-ANEPPS were perfused for 30 min after the hearts were stabilized in the Langendorff setup. Di-8-ANEPPS (10 µg) was prepared with 20 µl of 20% Pluronic (Biotium) in 5 ml of Tyrode's solution. Rhod-2AM (50 µg) was diluted with 20 µl of 20% Pluronic in 500 µl of Tyrode's solution and perfused at room temperature using peristaltic pumps. Stepwise details of the preparation of these dyes have been published by our group (Aguilar-Sanchez et al., 2017). A Peltier unit was used to set the temperature of the Tyrode's solution in the horizontal chamber to 33°C.

Experimental setup

Pressure measurements

We developed a novel experimental approach to study cardiac mechanics. The Langendorff perfused heart is a retroperfused preparation. Consequently, the pressure cannot be measured in the aorta. The usual approach to overcome this problem is to introduce a small balloon through the mitral valve and measure the pressure using a transducer. Here, we present a novel method in which we introduce a tiny vitrectomy ophthalmic-valved trocar (Alcon) in the apex of the left ventricle. The pressure at the outlet of the valve was measured with a solid-state integrated pressure transducer (Honeywell). A scheme of the methodology is presented in Fig. 1. Fig. 1 A shows how the ophthalmic-valved trocar is inserted though the apex of the left ventricle. Fig. 1 B illustrates the general arrangement used to measure the left intraventricular pressure. The trocar is connected through a valved coupler and is directly connected to the pressure transducer. The end-diastolic volume and the end-diastolic pressure can be imposed to the heart with the help of a column connected to the valved coupler through a fast electrovalve. Consequently, the height of the column will set the end-diastolic pressure when the electrovalve is open. The end-diastolic pressure can be modified by changing the height of the water column. The electrovalve will define the type of pressure measurement: if the electrovalve is closed, the measurement will be isovolumetric, and if it is open, it will be isotonic at constant load condition. Fig. 1 C depicts typical recordings of the isotonic pressure when end-diastolic pressure was modified. The pressures were calibrated before each experiment by plotting the pressure transducer output as a function of the column height. The inset illustrates how fast the developed pressure changes when the end-diastolic pressure is increased from a resting condition. Fig. 1 D shows a typical Frank–Starling response when the end-diastolic volume was increased. The increase in the end-diastolic volume produces an increase in the end-diastolic pressure (green dots). Interestingly, the developed systolic pressure (orange dots) presents a much larger increase than the diastolic pressure (green dots). This result is consistent with an increase in the diastolic pressure as function of the preload. Finally, measurements of the ventricular pressure using a plastic or latex balloon are usually obtained under isovolumetric conditions. In this article, we decided to evaluate the developed systolic pressure when the volume of the ventricle is changing (isotonic contraction). Compared with an isovolumetric contraction, this condition is closer to what happens with the ventricular function when blood is ejected from the ventricle. Finally, constant load implies that the height of the water (Tyrode's) column against which the heart is pumping out the ventricular volume and the output resistance are constant.

Electrical measurements using sharp microelectrodes and ECG

Sharp glass microelectrodes, filled with 3 M KCl, were used to record electrical signals during APs. An electrometric amplifier (WPI) was used to record the membrane potential. Glass microelectrodes were pulled with a Micropipette Puller (Flaming/Brown; Sutter Instrument Co.) and kept overnight in 3 M KCl to remove any air bubbles that could cause additional resistance or noise. These microelectrodes had a resistance of 10–20 MΩ. Microelectrodes were connected to a high input impedance differential amplifier (Duo 773 Electrometer; WPI) and positioned at the surface of the heart using a manual mechanical

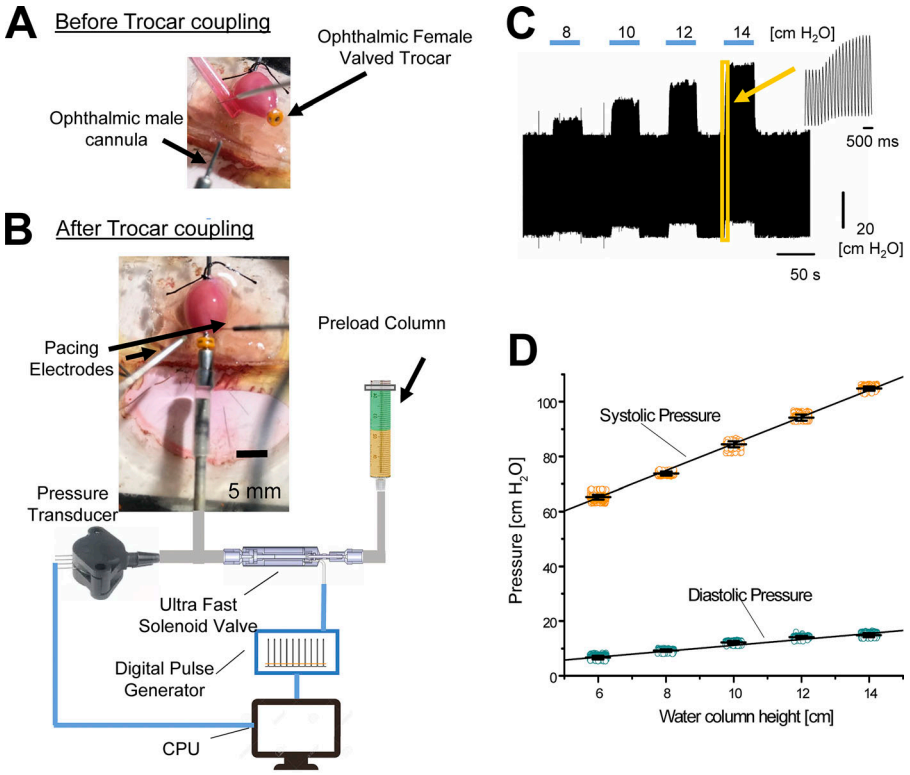

Figure 1. **Methodology for intraventricular pressure measurements. (A)** Positioning of the trocar in the apex of the left ventricle before the connection to the valve cannula. **(B)** Instrumentation arrangement to measure the ventricular pressure at different end-diastolic pressures. **(C)** A typical representative trace of the left ventricular pressure at different preloads. **(D)** A typical relationship between the diastolic (green circles) and systolic (orange circles) pressures for different preloads.

micromanipulator. Before the microelectrode was impaled on the tissue, the readout was adjusted to zero. The optically recorded APs were calibrated with the recordings from the microelectrodes. ECG traces were recorded transmurally, having one electrode inside the left ventricle and the other outside, with a DC-coupled amplifier.

The time course of AP was modified by blocking L-type Ca^{2+} channels with 10–20 µM of nifedipine in the perfusion solution. Either the I_{to} blocker 4-AP or the I_{to}-activator NS5806 was also added to the perfusion solution.

Pulsed local-field fluorescence microscopy (PLFFM)

The PLFFM technique has been used by our laboratory to assess physiological parameters by exciting exogenous fluorescent probes and detecting the light emitted by these indicators present in the tissue (Mejía-Alvarez et al., 2003; Valverde et al., 2010; Ferreiro et al., 2012; Kornyeyev et al., 2012). In PLFFM, the excitation and emitted light propagate through a multimode optic fiber placed on the surface of the heart. In this article, a beam splitter allowed us to use two optic fibers, which facilitated the recording of fluorescence from two distinct anatomical regions of the heart. The recording of two regions allowed us to do a comparative study of physiological properties, $[Ca^{2+}]$ and membrane potential, in different places within the intact heart.

PLFFM allowed us to evaluate the dynamics of $[Ca^{2+}]$ and membrane potential at different histological layers in the intact heart. To study the temporal propagation and/or spatial distribution of physiological signals, the fluorescence from multiple sites needed to be recorded simultaneously. The light source is a green, 532-nm, solid-state neodymium-doped yttrium-aluminum-garnet laser (Enlight Technologies). For transmural measurements, this light was split with a beam splitter to allow two 200-µm multimode optical fibers (0.67 numeric aperture) to illuminate the two layers of the ventricular wall. The beam was diverged using a beam expander or aspheric lenses. The expanded beam was reflected with the aid of a dichroic mirror onto a microscope objective. The objective focused the light beam into an optical fiber that was in contact with the tissue. For endocardial measurements, we made a small incision on the surface of the left ventricular free wall, facilitating the placement of the fiber onto the endocardium.

Loose-patch photolysis (LPP)

LPP allows the measurement of currents in an intact tissue during triggered physiological APs (Ramos-Franco et al., 2016). This experimental approach put together into one setup other techniques previously developed by our group. This includes PLFFM (Mejía-Alvarez et al., 2003; Valverde et al., 2010; Ferreiro et al., 2012; Kornyeyev et al., 2012), photo-breaking compounds with ultraviolet (UV) pulsing (Morad et al., 1983; Gurney et al., 1985; Sanchez and Vergara, 1994; Escobar et al., 1997, 2012), microelectrode measurements, and loose-patch recordings (Almers et al., 1984; Roberts and Almers, 1984).

The loose-patch pipette was made with a giant glass patch pipette using capillary tubes (WPI). These glass capillaries were heated with a torch to decrease the diameter size of one end to ~200 µm, allowing the fiber optic placed at the tip of the capillary to fill most of the patching area. This fiber was used to record intracellular Ca^{2+} or potentiometric signals at the loose-patch location or to provide small UV pulses to break photosensitive compounds and immediately assess resulting membrane currents (Ramos-Franco et al., 2016). The giant patch pipette

was filled with Tyrode's solution and held by a microelectrode holder half-cell (WPI). A micromanipulator was used to place the patch pipette on the surface of the ventricle. The interior of the giant glass patch pipette was voltage clamped to the same potential of the surrounding bath. A flash photolysis system let us fractionally change a specific ionic current (i.e., Ca^{2+} currents by photolyzing nifedipine) under the loose-patch pipette. Nifedipine was locally photoinactivated by UV illumination generated by a diode-pumped solid-state UV laser (355 nm). UV light was optomechanically shuttered for 1–50 ms and applied through an external quartz multimode fiber-optic or by a fiber positioned inside the patch pipette. The basic idea is to record the total membrane current with a macro patch pipette under conditions in which we can photolytically activate a conductance. The difference between the total current recorded in the presence and the absence of the drug allows us to reveal the specific current that was pharmacologically blocked. As the area under the pipette, where the current is recorded, is much smaller than the space constant, the neighboring tissue imposes an electrotonic coupling. This electrotonic coupling will act as an electric sink and impedes the activation of the photolitically activated current from producing any changes in the local AP beneath the recording pipette. This situation, in which a change in the transmembrane current there does not produce a change of the membrane potential, mimics what happens under a voltage-clamp condition, but in this case, the ventricular syncytium is acting as a spatial clamp. Finally, hearts were paced at 4–6 Hz and 33°C.

Statistical analysis

The physiological recordings of the APs, ECG, Ca^{2+} transients, Ca^{2+} currents, and ventricular pressure were evaluated based on well-established parameters in the field of cardiac electrophysiology. To compare between recordings before and after drug retroperfusion, the APs and Ca^{2+} transient traces were normalized to the mean value of the control signals.

The AP trace for each set of experiments was evaluated at certain repolarization times. Specifically, the time it takes for the AP to reach 30% or 90% repolarization (APD30 or APD90) was assessed. The repolarization times between control and noncontrol experiments were then evaluated and normalized to the control values for each heart. After this normalization, values from five experiments (n = 5 hearts, or otherwise noted) were compiled. Statistical analysis was performed with Origin 8 using one-way ANOVA.

Several parameters of Ca^{2+} transient kinetics were measured. Specifically, we measured the fractional Ca^{2+} transient amplitude with respect to a control trace; the rise time of the Ca^{2+} transients, measured as the time it takes for the Ca^{2+} transient to go from 10% to 90% of the maximum amplitude; and the half relaxation time, measured as the time it takes for the Ca^{2+} transient to relax to half of its maximum amplitude. Each of these parameters recorded in control and noncontrol experiments was evaluated and normalized to the control values for each heart used. The data from all the Ca^{2+} transients obtained from five experiments (n = 5 hearts unless stated otherwise) were compiled, and statistical analysis was performed with Origin 8 and one-way ANOVA.

Results

4-AP–sensitive Kv channels define mechanical and electrophysiological properties on an intact beating mouse heart

In mice, I_{to} has a central role in repolarizing the AP. Thus, we decided to test the hypothesis that alterations in this current will have a dramatic effect on cardiac contractility at the intact heart level. To test this idea, we performed experiments measuring the time course of the developed pressure in the left ventricle when I_{to} is blocked with increasing concentrations of the Kv blocker 4-AP.

Fig. 2 illustrates a typical experiment in which I_{to} was impaired with different concentrations of 4-AP. As we show in Fig. 2 A, even a low concentration of 4-AP (10 µM) can produce a significant increase in the amplitude of the ventricular developed pressure under an isotonic condition at a constant afterload. The inset in Fig. 2 A illustrates the effect of 300 nM of isoproterenol on the pressure measured with the new method in which a vitrectomy ophthalmic-valved trocar was introduced in the left ventricle. This indicates that this new method can track increases in the developed pressure under different experimental conditions that promote an increase in contractility. In Fig. 2 B, we can observe the change in the amplitude of the systolic pressure upon retroperfusion with increasing concentrations of 4-AP. Specifically, a short 12-s bolus of 4-AP dissolved in Tyrode's solution was applied through the coronary vasculature. At all concentrations, we can observe a significant increase in systolic pressure that decreases to values similar to the control condition when 4-AP is washed out. This protocol allowed us to construct a dose–response curve (Fig. 2 C) showing that there were significant increases of the measured pressure for each concentration of 4-AP (n = 5 hearts) and that the effect of 4-AP on contraction has an 50% inhibitory concentration of 21.9 ± 1.5 µM.

Although the reported affinities for the blocking of Kv 4.2 and Kv 4.3 by 4-AP are ∼1 mM, in the experiments presented in Fig. 2, a much lower 4-AP concentration showed a large effect on the developed pressure, suggesting that other Kv channels can control contractility. Consequently, to assess if low concentrations of 4-AP have an impact on ventricular electrical activity, we decided to evaluate the effect of 4-AP in the repolarization of the epicardial AP.

Recently, we demonstrated that although the mouse epicardial AP displays a fast phase 1, it also shows a significant phase 2 at a more hyperpolarized (more negative) membrane potential compared with other mammals when recordings are made at the intact heart level under physiological conditions. Interestingly, phase 2 is not directly driven by an influx of Ca^{2+} through L-type Ca^{2+} channels, but by the influx of Na^{+} through the NCX. Fig. 3 shows the effect of 4-AP on the repolarization of the epicardial AP. Fig. 3 (A–C) depicts the action of the blocker when a heart was perfused with increasing concentrations of 4-AP. In the three cases (Fig. 3, A–C), the AP shows a typical epicardial spike-and-dome behavior. Additionally, it is possible to observe that the application of 4-AP slows phase 1 repolarization and prolongs AP duration. The APD30 was evaluated during the application of increasing concentrations of 4-AP, inducing

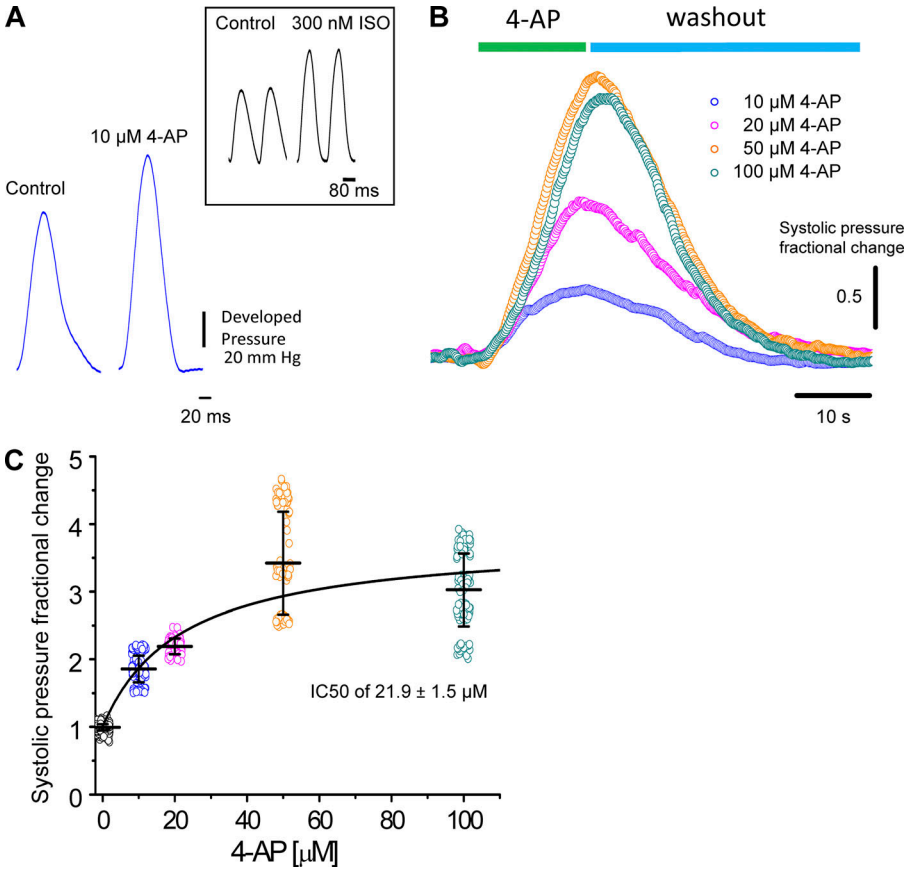

Figure 2. **4-AP increases the developed ventricular systolic pressure in intact mouse hearts. (A)** Time course of the developed pressure during the cardiac cycle in the absence (control) and presence of 10 µM 4-AP. Inset illustrates the increase in the developed pressure induced by 300 nM of the positive ionotropic agent isoproterenol (ISO). **(B)** Plot of the evolution of the developed systolic pressure peak value upon perfusion with different concentrations of 4-AP. The 4-AP–containing solutions were retro-perfused through the coronary circulation. A 12-s application of 4-AP significantly increased the systolic pressure. This pressure response recovered to the initial systolic pressure when 4-AP was washed out. **(C)** Dose–response curve for different concentrations of 4-AP. All the tested 4-AP concentrations induced a significant increase in the systolic pressures (peak of the developed pressure, 1,099 total measurements) with respect to the control condition. *n* = 5 hearts.

prolongation of APD30 (Fig. 3 D). Interestingly, when the APD90 was computed, the fractional increase of APD90 was smaller than that of APD30. Indeed, 10 µM of 4-AP can induce an increase of 52% in APD30 and 8.4% in APD90. This indicates that channels blocked by 4-AP mostly define the early fast repolarization during phase 1.

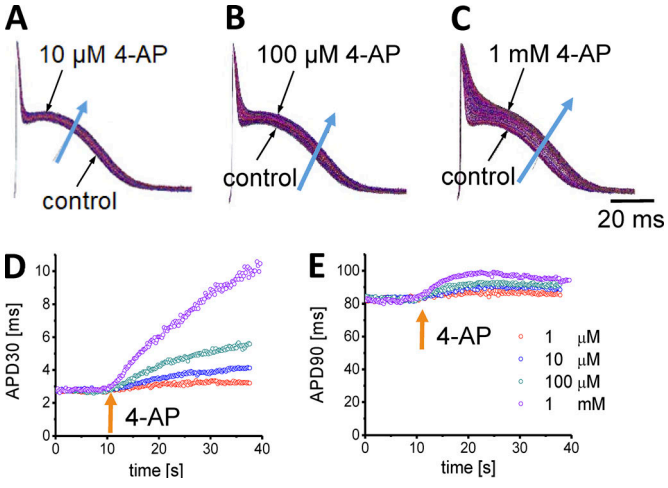

Figure 3. **4-AP application induces a larger increase on APD30 than on APD90. (A–C)** Consecutive recordings of epicardial ventricular AP upon perfusion with different concentrations of 4-AP. The black arrows indicate the beginning and end of 4-AP perfusion. The blue arrows indicate the direction of the [4-AP] increase. Note that [4-AP] does not increase instantaneously due to the rate limited coronary and capillary perfusion. **(D and E)** The effect of different 4-AP concentrations on AP repolarization evaluated by assessing the APD30 and APD90 of consecutive epicardial APs. It is possible to observe that the effect on APD30 is significantly larger than on APD90.

Although low concentrations of 4-AP have a profound effect on the mechanical response and AP repolarization, it is difficult to relate these two variables, because the pressure is a global variable and the latter is a local variable (epicardial repolarization). Moreover, it is difficult to determine how much the epicardium contributes to the global electrical activity. Therefore, to evaluate a global electrical variable, we decided to measure the waveform ECG signals. Interpreting ECGs in a mouse heart has traditionally been a challenging problem. For example, in large mammals such as humans, the T wave represents the difference in the repolarization time between epicardium and endocardium. In contrast, in the mouse, the T wave reflects the difference in timing between the repolarization of the apex and the repolarization of the base. However, when the ECG was transmurally recorded (with one electrode in the left ventricular chamber and a second one outside the left ventricular epicardial layer), the mouse T wave showed the temporal difference in the transmural repolarization as in larger mammals. Furthermore, the transmural ECG is an ideal tool to explore the J wave produced because of the kinetic difference in phase 1 repolarization between epicardium and endocardium. Fig. 4 A illustrates a simultaneous recording of an epicardial AP and the corresponding transmural ECG. It is possible to observe that the QRS complex appears before the epicardial depolarization because the endocardium depolarizes before the epicardium. In addition, the T

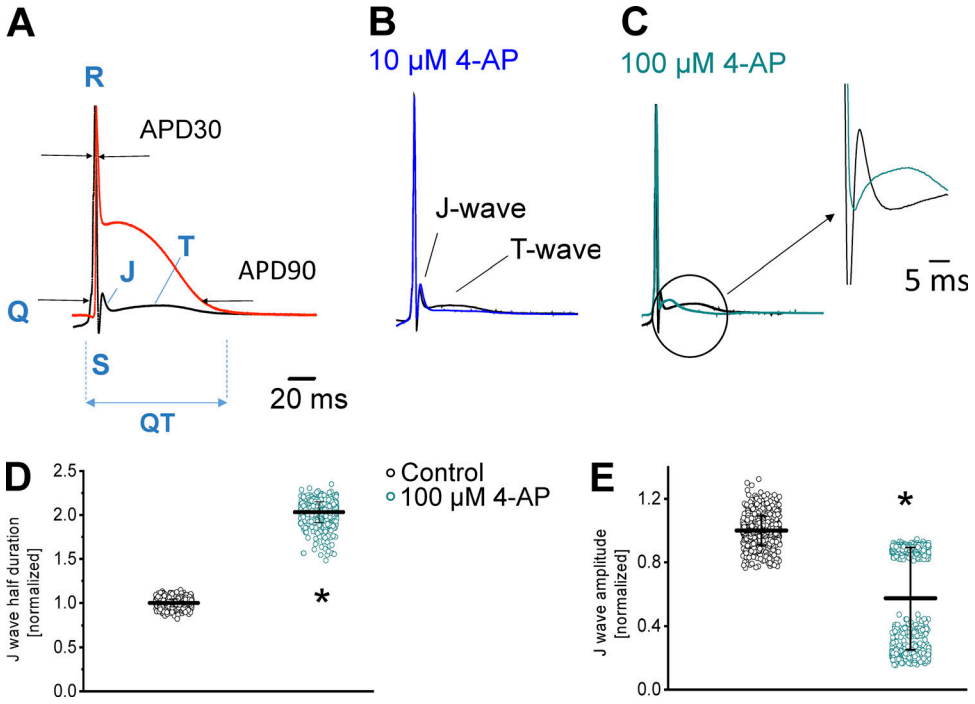

Figure 4. **Effect of 4-AP on the left ventricle transmural ECG signal. (A)** Superimposed epicardial AP (red trace) and transmural ECG (black trace) recorded from the left ventricle. It is possible to appreciate that the J wave reflects the fast repolarization during phase 1 and the T wave coincides with phase 3. The black arrows indicate the position where APD30 and APD90 were evaluated. **(B and C)** The effect of two different concentrations (10 and 100 µM) of 4-AP on transmural ECG recordings. Inset of C: 4-AP reduces the amplitude and increases the duration of the J wave (dark cyan trace) relative to control (black trace). Thus, the perfusion with 100 µM 4-AP reduces the left ventricle transmural repolarization gradient. **(D)** Measurements of the J wave half duration in the presence of 100 µM 4-AP. The drug significantly spread out the J wave (1.0 ± 0.04, 1,065 measurements for the control condition, black circles; vs. 2.03 ± 0.11, 870 measurements for 4-AP, dark cyan circles). **(E)** Measurements of the J wave amplitude of four different ECG experiments. Although there is scattering in the data, it is possible to observe that 4-AP has a large effect on J wave amplitude (1.0 ± 0.09, 675 measurements for the control condition, black circles; vs. 0.57 ± 0.32, 891 measurements for 4-AP, dark cyan circles). For all the experiments, the population means between control and the perfused hearts with 100 µM 4-AP were significantly different (*, $P < 0.001$). *n* = 4 hearts.

wave coincides with the phase 3 AP repolarization. What is more remarkable is that the J wave emerges during the fast phase 1 repolarization, making the evaluation of this wave a precise way to assess the fast repolarization during phase 1 at different transmural levels. Fig. 4 (B and C) shows the effect of 10 and 100 µM of 4-AP on the J wave amplitude and kinetics. As shown in the inset of Fig. 4 C, 4-AP clearly induced an increase in the J wave duration and a decrease in the J wave amplitude. Fig. 4 D presents the effect of 100 µM of 4-AP on the half duration of the J wave from five different hearts. 4-AP produced a significant increase (at the 0.001 level) in the J wave half duration of 100.3 ± 11%. Additionally, 100 µM of 4-AP produced significant decreases (at the 0.001 level) in the amplitude of the J wave of 43 ± 32% in four different independent hearts (Fig. 4 E). Altogether, experiments presented in Fig. 4 suggest that 4-AP has not only an effect on the rate of phase 1 repolarization (J wave half duration) but also a differential effect on epicardial and endocardial repolarization. Indeed, a decrease in the amplitude of the J wave indicates that the difference between the epicardial and endocardial rates of phase 1 repolarization has decreased.

Even though the amplitude and the kinetics of the J wave reflect how the early phase 1 repolarization is occurring across the ventricular wall, it is not possible to exactly infer how 4-AP is modifying the AP repolarization in the endocardium. Assessing the kinetics of AP repolarization in the epicardium and the endocardium simultaneously in an intact perfused heart has been experimentally difficult.

The block of 4-AP–sensitive Kv channels have a larger effect in controlling electrophysiological and Ca^{2+} signaling properties in the epicardium than in the endocardium

Recently, our group reported for the first time the assessment of epicardial and endocardial APs using potentiometric dyes and a dual PLFFM. The idea is to retroperfuse a beating heart through the coronary bed with the potentiometric dye Di-8-ANNEPS. This approach allows a homogeneous loading of cardiac myocytes across the ventricular wall. After the heart is loaded with the dye, we use two independent high-numerical-aperture optical fibers attached to a PLFFM to record changes in membrane potential reflected as the changes in the dye-emitted fluorescence.

PLFFM allows the assessment of electrophysiological parameters and Ca^{2+} signaling properties across the ventricular wall. A typical experiment in which epicardial and endocardial AP were simultaneously recorded is presented in Fig. 5 A, where three main features can be observed. First, the endocardium depolarizes before the epicardial layer. This is responsible for the positive QRS complex presented in Fig. 4 A. Second, the early

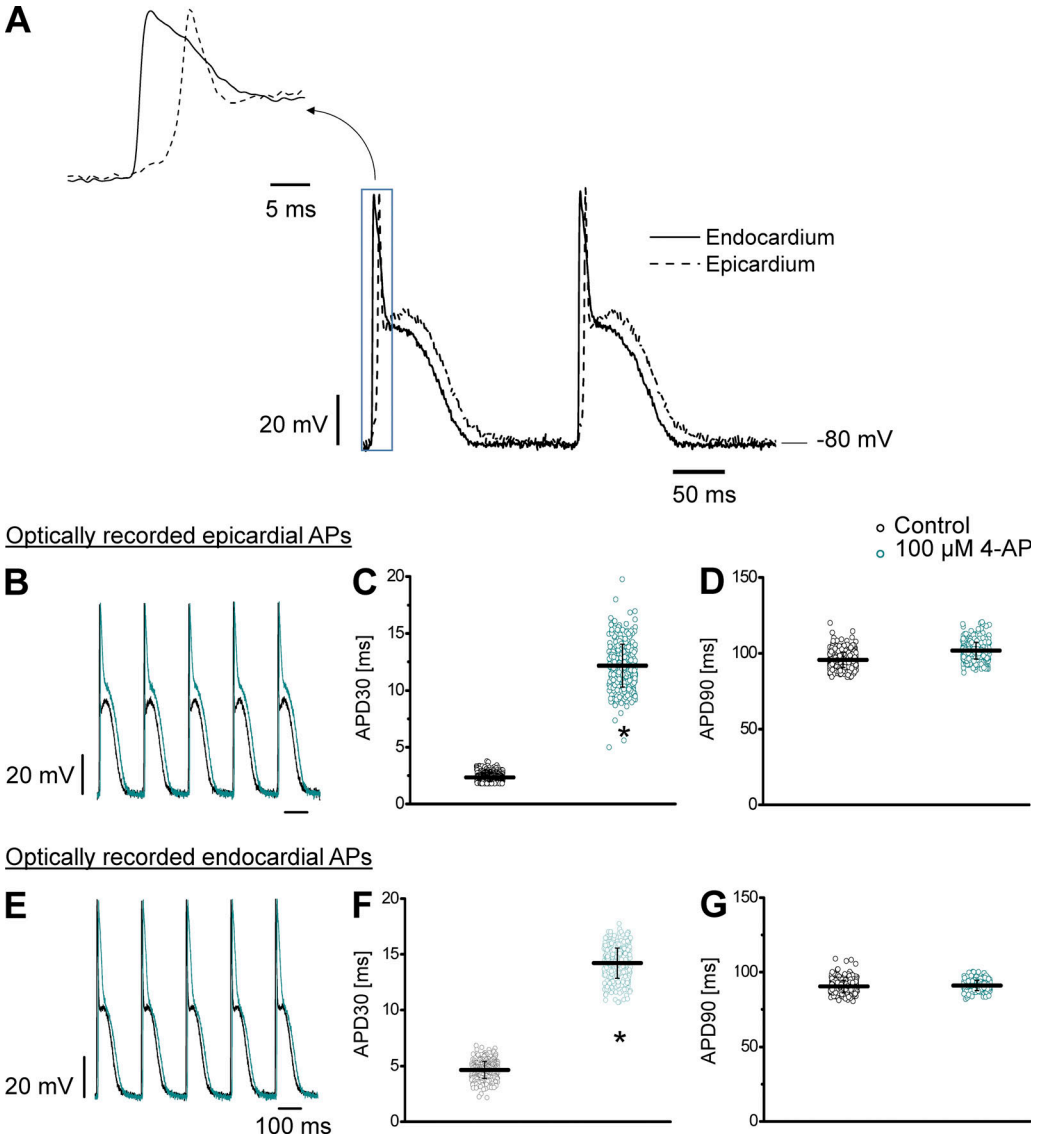

Figure 5. **Differential effect of 4-AP on simultaneous epicardial and endocardial optically recorded APs. (A)** The kinetic differences between epicardial and endocardial APs recoded simultaneously on an intact perfused heart. It is possible to observe the differences in the kinetics of these transmurally recorded APs. In the inset, we can see that there is not only a delay between the endocardial and the epicardial APs, but also that the rate of repolarization during phase 1 is slower in the endocardium. **(B and E)** The effect of 100 µM 4-AP (dark cyan traces) on the kinetics of epicardial and endocardial AP, respectively. **(C and F)** The distribution of the APD30 measurements of epicardial and endocardial APs before and after the application of 100 µM 4-AP. 4-AP induces a significant decrease in the rate of repolarization. Interestingly, there are statistically significant differences (*) in the APD30 ($P < 0.001$) between endocardium (4.65 ± 0.76 ms, 377 measurements, black circles; F) and epicardium (2.34 ± 0.37 ms, 376 measurements, black circles; C) before the application of the drug. However, this statistically significant difference between endocardium and epicardium disappears when the hearts are perfused with 100 µM 4-AP (14.21 ± 1.36 ms, 499 measurements, dark cyan circles, F vs. 12.17 ± 1.88 ms, 499 measurements, dark cyan circles; C). **(D and G)** The perfusion with 100 µM 4-AP does not induce statistically significant changes at the APD90 level ($P < 0.001$) for epicardium (95.62 ± 4.95 ms, 494 measurements, black circles; vs. 101.75 ± 5.53 ms, 497 measurements, dark cyan circles; D) and endocardium (90.34 ± 4.21 ms, 374 measurements, black circles vs. 90.93 ± 3.33 ms, 499 measurements, dark cyan circles; G). n = 10 hearts.

repolarization during phase 1 is slower in endocardium than in epicardium (4.66 ± 0.76 ms vs. 2.35 ± 0.37 ms, n = 10 hearts). This difference in kinetics is key in determining the J wave in the mouse heart. Finally, the epicardial layer presents a prominent spike-and-dome morphology, an experimental observation presented in several mammalian models. As epicardium and endocardium display significant differences in the early repolarization kinetics, we decided to evaluate the effect of blocking Kv channels with 4-AP on each layer. As was shown in Fig. 3, 4-AP has a larger effect on the APD30 of the epicardial AP (Fig. 5 C) than on the APD90 (Fig. 5 D). Interestingly, although 4-AP also slows down the rate of repolarization in the endocardium (Fig. 5, E and F), the effect on the phase 1 repolarization rate is smaller in the endocardium than on the epicardial AP (Fig. 5, B and C). Indeed, the ratios of the APD30 in the absence and presence of 100 µM 4-AP were 5.3 times in epicardium versus 3 times in endocardium. This lower sensitivity in the endocardium can reflect the lower expression of Kv 4.x in this

internal ventricular layer (Mattiazzi et al., 2015; Aguilar-Sanchez et al., 2017).

Undoubtedly, the perfusion of the hearts with 4-AP has a dramatic effect on both the mechanical and electrical properties of the mouse heart. However, none of the experiments presented above define the relationship between excitability and contractility. Therefore, we designed experiments to directly evaluate how changes in the AP waveform can modify the systolic Ca^{2+}. The most likely scenario is that 4-AP will enhance Ca^{2+} release from the SR by changing the amplitude and the kinetics of the L-type Ca^{2+} currents. In addition, if 4-AP has an effect on the amplitude of Ca^{2+} transients, we expect that 4-AP will have a larger effect on the epicardium than in the endocardium. To assess the effect of 4-AP on the amplitude of the Ca^{2+} transients in the epicardium and the endocardium, we performed experiments to measure simultaneously Ca^{2+} transients in both layers. The Ca^{2+} transient recordings were obtained by perfusing the heart with the Ca^{2+} indicator Rhod-2 and by simultaneously recording fluorescence signals with two independent optical fibers coupled to a PLFFM. Experiments presented in Fig. 6 illustrate the effect produced by the perfusion of the heart with 100 µM 4-AP on the amplitude and the kinetics of epicardial and endocardial Ca^{2+} transients (n = 4 hearts). Fig. 6 (A–D) shows that 4-AP induces an increase in the amplitude, rise time, and half relaxation time of the epicardial Ca^{2+} transients. Even more, although 4-AP also induces an augmentation of the amplitude and the duration of the endocardial Ca^{2+} transients (Fig. 6, E–H), the effect on this innermost layer is smaller than in the epicardium. This is consistent with the idea that the epicardial effects of 4-AP are larger due to the heterogeneous expression of Kv 4.x channels across the ventricular wall.

Clearly, the results presented in Fig. 6 demonstrate that the increase in the systolic pressure with 4-AP observed in Fig. 2 is due to an increase in the amplitude and the kinetics of the Ca^{2+} transient. However, we still miss the link between the decreased rate of repolarization during phase 1 and the increase in cytosolic Ca^{2+} (contractility). As we already stated, the most likely possibility is that changes in the AP phase 1 repolarization will induce an increase in the amplitude of the L-type Ca^{2+} current and the total amount of Ca^{2+} that this transport mechanism brings into the cells. Recently, our laboratory was able to measure for the first time Ca^{2+}-dependent currents during a triggered AP at the intact heart level using the novel LPP technique (Ramos-Franco et al., 2016). To assess if changes during the repolarization of phase 1 can define the kinetics of Ca^{2+} influx into the cell, we performed LPP experiments in hearts exposed to 4-AP. A typical experiment is shown in Fig. 7 (A and B), which illustrates epicardial currents recorded in the absence and presence of 100 µM 4-AP, respectively. The LPP recording shows two components, one fast early current and a late slower current. As we already demonstrated in a previous article (Ramos-Franco et al., 2016), the current during the early phase is carried by Ca^{2+} ions permeating through L-type Ca^{2+} channels, and the late component is mediated by the influx of Na^+ through the NCX acting in its forward mode. Furthermore, in Ramos-Franco et al. (2016), we demonstrated that this Ca^{2+} influx was terminating by voltage-dependent deactivation and not by Ca^{2+}-dependent inactivation.

This late Na^+ current through the NCX is activated by Ca^{2+} released from the SR. Remarkably, the perfusion of the heart with 4-AP not only induces an increase in the amplitude of the fast inward component of the current but also increases its mean duration. Fig. 7 (C and D) reinforces this observation: currents recorded from five different animals show that the increase in the current amplitude and the total charge carried through the L-type Ca^{2+} currents during phase 1 of the AP is significantly larger in hearts perfused with 4-AP (57% for the total charge) than in control hearts.

One critical aspect of LPP experiments is to record simultaneously the transmembrane current and the epicardial AP. This allows us to verify if the photolytic activation of the inward current is changing the properties of the AP.

As we already demonstrated, perfusion of the heart with nifedipine induces a reduction in the amplitude of phase 2 (Ferreiro et al., 2012). In addition, we found that in the presence of nifedipine, the effect of 4-AP on the phase 1 repolarization rate was much smaller. Fig. 8 A illustrates the effect of 4-AP in the presence of nifedipine in the AP. Additionally, data obtained from five different hearts show that in the presence of nifedipine, 4-AP's effect was 4 times smaller (Fig. 8, B and C). This result suggests that the repolarization kinetics during phase 1 is defined by a competition between a K^+ efflux and a Ca^{2+} influx (Gómez et al., 1997). Therefore, 4-AP will have a dual role in phase 1 repolarization. First, it will block Kv channels, slowing the rate of repolarization, and second, the slower repolarization will keep the membrane potential depolarized for a longer time during phase 1. This will reduce the deactivation of the L-type Ca^{2+} channel. This "prolonged activation" (increase in the open probability) not only will bring more Ca^{2+} into the cell to increase contractility but also will modify the AP repolarization.

Activation of Kv 4.x channels reduces the mechanical response by increasing the rate of repolarization during phase 1; this finally leads to an attenuation in the L-type Ca^{2+} and the Ca^{2+} transient

Results presented in this article indicate that the blockage of Kv channels increases the systolic force because a slower AP repolarization phase 1 increases the Ca^{2+} influx through L-type channels, activating a larger Ca^{2+} transient with the concomitant increase in contractility. A final proof of concept supporting this idea is the assessment of contractility (i.e., Ca^{2+}) when the Kv channels are activated instead of being inhibited. Kv channels are tetramers in which each α subunit has six transmembrane segments. Although this is the main structure for K^+ permeation, other regulatory subunits can modify the level of expression and also can regulate the kinetics of the channels. Moreover, a central regulatory subunit, K^+ channel-interacting protein (KChIP), has a central role in regulating the Kv 4.x channels. Furthermore, some drugs can interact with Kv 4.x channels when KChIP is also expressed in the plasma membrane. Interestingly, NS5806 can slow the rate of inactivation of Kv 4.x when the α subunit interacts with KChIP (Gonzalez et al., 2014). Thus, we expect that NS5806 will accelerate the rate of

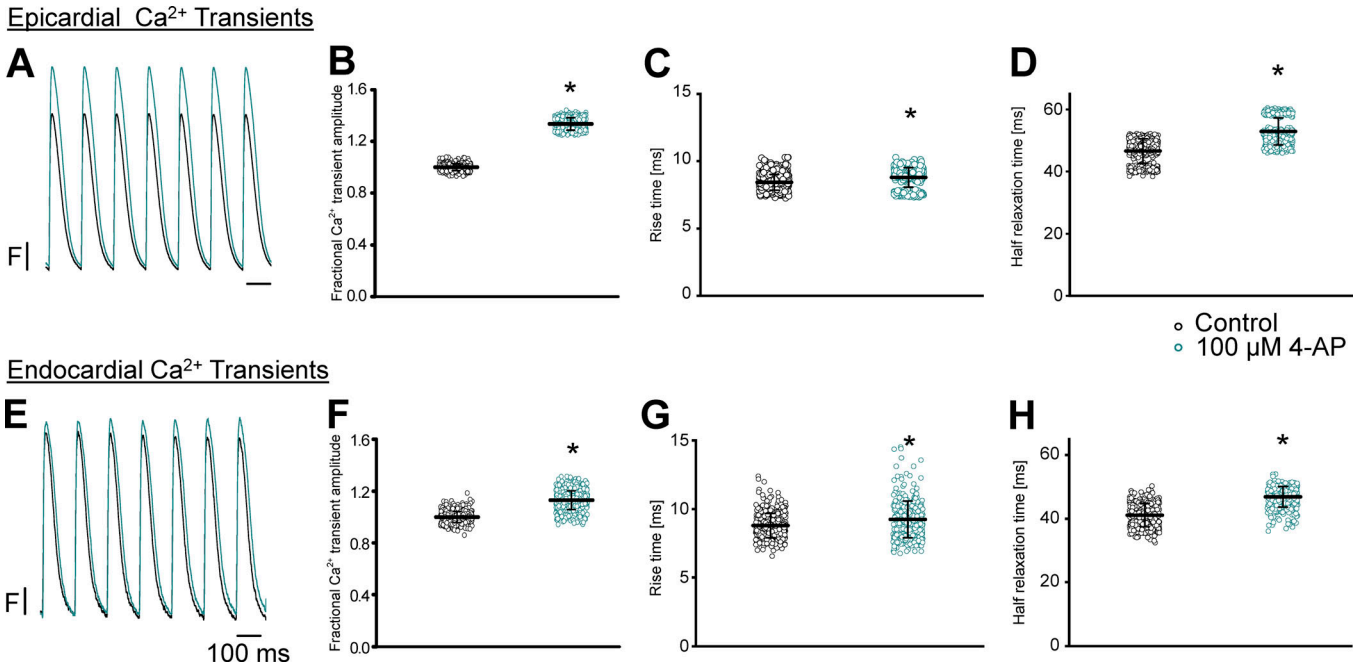

Figure 6. **4-AP has a larger effect on epicardial than on endocardial Ca^{2+} transients. (A and E)** The effect of 100 µM 4-AP on the amplitude and the kinetics of Ca^{2+} transients recorded simultaneously in epicardium and endocardium when the heart was externally paced at 7 Hz. **(B–D)** The effect of 100 µM 4-AP on different parameters of epicardial Ca^{2+} transients. **(E and F)** 100 µM 4-AP has a significant effect (*) on the amplitude of endocardial Ca^{2+} transients. However, if we compare the magnitude of the effect of 100 µM 4-AP on endocardium (F; dark cyan circles) versus epicardium (B; dark cyan circles), the effect in endocardium is significantly smaller (1.13 ± 0.07 times, 588 measurements, dark cyan circles; E vs. 1.33 ± 0.04 times, 557 measurements, dark cyan circles; B). **(C and G)** 100 µM 4-AP has a significant effect (*, $P < 0.001$) on the rise time of the Ca^{2+} transients in the epicardium (8.42 ± 0.58 ms, 662 measurements, black circles vs. 8.78 ± 0.72 ms, 623 measurements, dark cyan circles; C) and the endocardium (8.79 ± 0.89 ms, 474 measurements, black circles vs. 9.24 ± 1.34 ms, 400 measurements, dark cyan circles; G). *n* = 4 hearts. **(D and H)** 100 µM 4-AP has a significant effect (*, $P < 0.001$) on the half relaxation time of the Ca^{2+} transients in the epicardium (46.5 ± 3.9 ms, 662 measurements, black circles vs. 52.9 ± 4.3 ms, 663 measurements, dark cyan circles; D) and the endocardium (41.11 ± 3.6 ms, 451 measurements, black circles vs. 46.92 ± 3.24 ms, 623 measurements, dark cyan circles; D). *n* = 4 hearts.

repolarization during phase 1. Fig. 9 illustrates experiments on epicardium that were designed to test this idea. Fig. 9 A shows that 10 µM NS5806 dramatically accelerates phase 1 repolarization (see inset) and decreases both the amplitude of phase 2 and the APD90. Statistical data obtained from five different hearts (Fig. 9, B and C) show significant changes in the APD30 and APD90 of epicardial AP.

If the prolongation of phase 1 induces an increase in contractility, we expect that an increase in the rate of repolarization will attenuate the amplitude of myoplasmic Ca^{2+} transients. Indeed, when the hearts were perfused with NS5806, there was a strong decrease of the heart mechanical activity. Fig. 10 A shows the time course of the normalized developed pressure in a heart that was perfused with 30 µM NS5806. A statistical analysis of the effect of NS5806 on the developed pressure is shown in Fig. 10 B (103.2 ± 6.7% for the control and 38.0 ± 5.5% for NS5806; *n* = 3 hearts). Moreover, Fig. 11 (A–D) reveals that the perfusion of murine hearts with 10 µM NS5806 induces a reduction in the amplitude, rise time, and half relaxation time and the duration of epicardial Ca^{2+} transients.

Furthermore, to unmask the molecular mechanism by which NS5806 reduces the amplitude of Ca^{2+} transient, we performed experiments to record the Ca^{2+} influx through L-type Ca^{2+} channels in the presence of 10 µM NS5806. Fig. 12 (A and B) shows that an increase in the magnitude of I_{to} decreases the amplitude of Ca^{2+} currents measured with LPP. Moreover, increasing the rate of repolarization not only affects the amplitude of the Ca^{2+} current but also decreases the duration of the current (Fig. 12, C and D). This effect seems to be a consequence of faster deactivation of the L-type Ca^{2+} current due to an increased rate of AP repolarization during phase 1.

Discussion

The results presented here demonstrate that the Ca^{2+} influx that triggers Ca^{2+} transients happens during phase 1 and that the kinetics of this fast repolarization can regulate contractility in mice. Mouse ventricular APs present notable differences compared with ventricular APs recorded from other species (Knollmann et al., 2001; Sah et al., 2003; Brunet et al., 2004; Ramos-Franco et al., 2016). The most distinguishable property is the appearance of a robust phase 1 during the early repolarization. This allows the mouse heart to beat at a remarkably high rate.

The idea that the phase 1 rate of repolarization could be involved in regulating contractility has been discussed by other authors (Bouchard et al., 1995; Volk et al., 1999; Sah et al., 2002). However, in this article, we were able to integrate, at the intact heart level under physiological conditions, the relationship

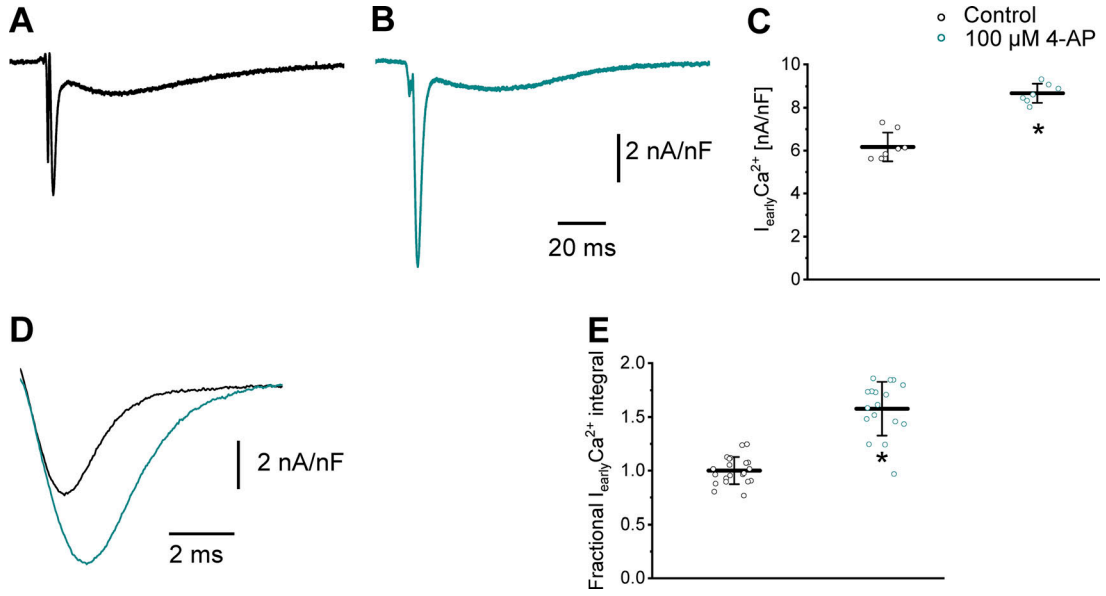

Figure 7. **The increase in contractility promoted by 4-AP is driven by an increase in the L-type Ca^{2+} current during phase 1. (A and B)** Time course of Ca^{2+}-dependent ionic currents recorded with LPP before (black trace) and after (dark cyan trace) the hearts were perfused with 100 µM 4-AP. **(C)** 4-AP increases the amplitude of the early Ca^{2+} current (6.16 ± 0.66 nA/nF, eight measurements, black circles vs. 8.67 ± 0.44 nA/nF, seven measurements, dark cyan circles). **(D and E)** 4-AP not only increases the amplitude of the early component but also increases its duration and time integral (1.13 ± 0.99 times, 21 measurements, black circles vs. 1.57 ± 0.25 times, 17 measurements, dark cyan circles). Results from five different hearts illustrate that the amount of Ca^{2+} that gets into the cell during 4-AP perfusion is significantly larger (*) respect to their controls at P > 0.001. *n* = 5 hearts.

between the rate of phase 1 repolarization, Ca^{2+} influx, and contractility across the ventricular wall.

This fast phase 1 is highly dominated by the activation of I_{to}. This current is encoded by two genes, Kv 4.2 and Kv 4.3 (Guo et al., 1999; Rossow et al., 2006, 2009; Teutsch et al., 2007; Huo et al., 2014). Although the activation of I_{to} has been historically linked with a transmural repolarization gradient, it has been reported that changes in the amplitude of this current can have a profound effect on the cardiac contractility of other species.

Fig. 2 shows that increasing concentrations of 4-AP can proportionally augment the systolic pressure. This result is consistent with mechanical shortening experiments in isolated myocytes described by several authors. For example, Kondo et al. (2006) showed that 100 µM 4-AP increases sarcomere shortening in isolated mouse myocytes from different

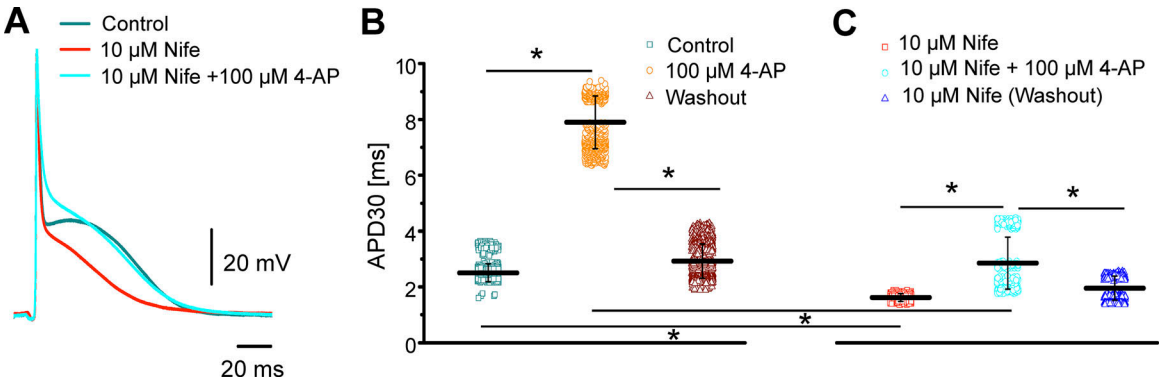

Figure 8. **L-type Ca^{2+} currents can define the rate of repolarization during phase 1. (A)** Effect of nifedipine (Nife; red trace) and 4-AP (cyan trace) on the time course of an epicardial AP. While 10 µM Nife alone induced a notorious effect on phase 2, Nife + 4-AP modified phase 1 and phase 2. **(B and C)** Summarized results from five different hearts. B shows that 100 µM 4-AP has a significant effect (*, P < 0.001) on APD30 (2.50 ± 0.32 ms, 1,654 measurements, light green squares vs. 7.89 ± 0.94 ms, 1,115 measurements, orange circles; B) that can be washed out (P < 0.001; 7.89 ± 0.94 ms, 1,115 measurements, orange circles vs. 2.92 ± 0.61 ms, 1,311 measurements, wine triangles; B). C shows that 100 µM 4-AP, in the presence of Nife, significantly increases (*, P < 0.001) APD30 (1.62 ± 0.14 ms, 398 measurements, red squares vs. 2.85 ± 0.92 ms, 368 measurements, cyan circles; C) and that this effect can be also washed out (P < 0.001; 2.85 ± 0.92 ms, 368 measurements, cyan circles vs. 1.95 ± 0.43 ms, 389 measurements, blue triangles; C). Nife not only significantly reduces (P < 0.001) the APD30 under control conditions (2.50 ± 0.32 ms, 1,654 measurements, light green squares; B vs. 1.62 ± 0.14 ms, 398 measurements, red squares; C) but also shows a significant effect (P < 0.001) in the presence of 100 µM 4-AP (7.89 ± 0.94 ms, 1,115 measurements, orange circles; B vs. 2.85 ± 0.92 ms, 368 measurements, cyan circles; C). *n* = 5 hearts.

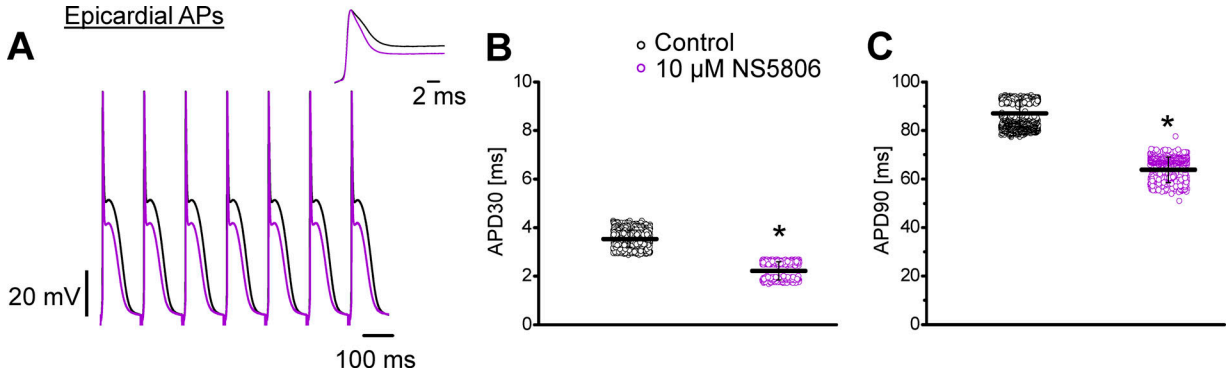

Figure 9. **NS5806 accelerates phase 1 repolarization. (A)** Effect of NS5806 on the time course of epicardial AP, where the black traces are the controls and the violet traces are in the presence of 10 μM NS5805. NS5806 shortened both APD30 (see inset) and APD90. **(B)** The significant effect (*, P < 0.001) of 10 μM NS5805 on APD30 (3.53 ± 0.34 ms, 1,059 measurements, black circles vs. 2.21 ± 0.37 ms, 808 measurements, violet circles). **(C)** The significant effect (*, P < 0.001) of 10 μM NS5805 on APD90 (87.06 ± 5.52 ms, 1,057 measurements, black circles vs. 63.73 ± 5.23 ms, 808 measurements, violet circles). *n* = 5 hearts.

ventricular regions. Dong et al. (2006) showed that in dogs (i.e., a larger mammal), a reduction in the rate of phase 1 repolarization also increases the degree of myocyte shortening. However, both sets of experiments, in mice and dogs, were performed in cells that were not under mechanical load, a condition that can significantly change the mechanical response of cardiac myocytes. The maximal systolic pressure measured in this article is lower than the ones reported by other authors (Said et al., 2008). Our pressure measurements were performed under isotonic conditions at a constant load. This experimental condition will always show lower systolic pressure values compared with isovolumetric recordings (Said et al., 2008), because the volume of the ventricle will be reduced during the contraction.

As it was already stated in Results, the most likely cause of an increase in the developed pressure during 4-AP perfusion is its effect on K^+ channels defining AP phase 1. Fig. 3 not only illustrates the increasing effect of 4-AP on the AP repolarization but also reveals that APD30 is significantly more affected than APD90. This result challenges the idea that submillimolar concentrations of 4-AP have a larger effect on APD90 than on APD30 (Kondo et al., 2006). Those authors proposed that at lower concentration, 4-AP has a greater effect on delayed rectifying K^+ currents (I_{Kur}, Kv 1.5) than on I_{to}. One possible explanation for the difference between our results and those reported by Kondo et al. is that the APs measured by them were obtained from ventricular myocytes under whole-cell current clamp conditions. This approach dramatically dampens phase 2 in mouse ventricular myocytes, a situation that enhances the effect of K^+ channel blockers on APD90. Furthermore, as we already established (Kornyeyev et al., 2010, 2012; Valverde et al., 2010; Ferreiro et al., 2012; Mattiazzi et al., 2015; Ramos-Franco et al., 2016; Aguilar-Sanchez et al., 2017), APs recorded from different ventricular regions of an intact perfused heart always display a predominant phase 2. Thus, in APs recorded ex vivo at the intact heart level, 4-AP has only a small effect on APD90 due to the presence of phase 2.

Additionally, other authors (Fiset et al., 1997) have shown that micromolar concentrations of 4-AP block Kv 1.5 channels. They demonstrated that low concentrations of 4-AP slow down AP phase 1 in isolated myocytes and increase the developed pressure in AP recorded at room temperature. By contrast, others (Li et al., 2001) demonstrated that at 35°C, the overexpression of Kv 1.5 does not modify the rate of repolarization

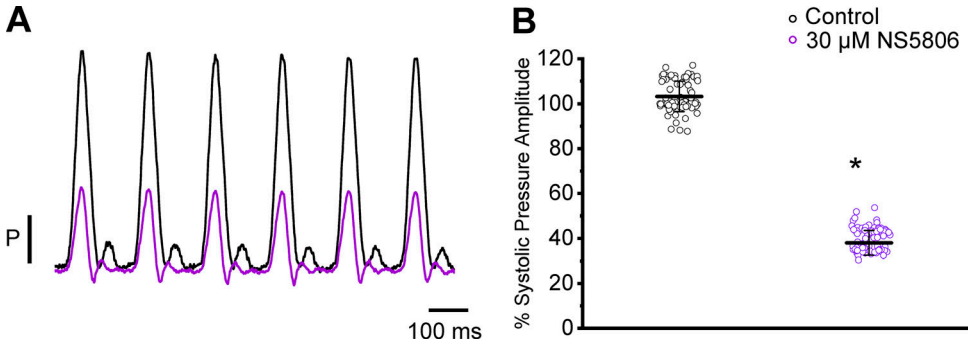

Figure 10. **NS5806 decreases the left ventricle developed pressure. (A)** Time course of the left ventricle developed pressure during an isotonic contraction at a constant afterload before (black trace) and after (violet trace) perfusion with 30 μM NS5806. **(B)** The significant effect (*, P < 0.001) of NS5806 on the normalized developed pressure (103.3 ± 6.7%, 85 measurements for the control, black circles vs. 38.03 ± 5.48%, 125 measurements for NS5806, violet circles). *n* = 3 hearts.

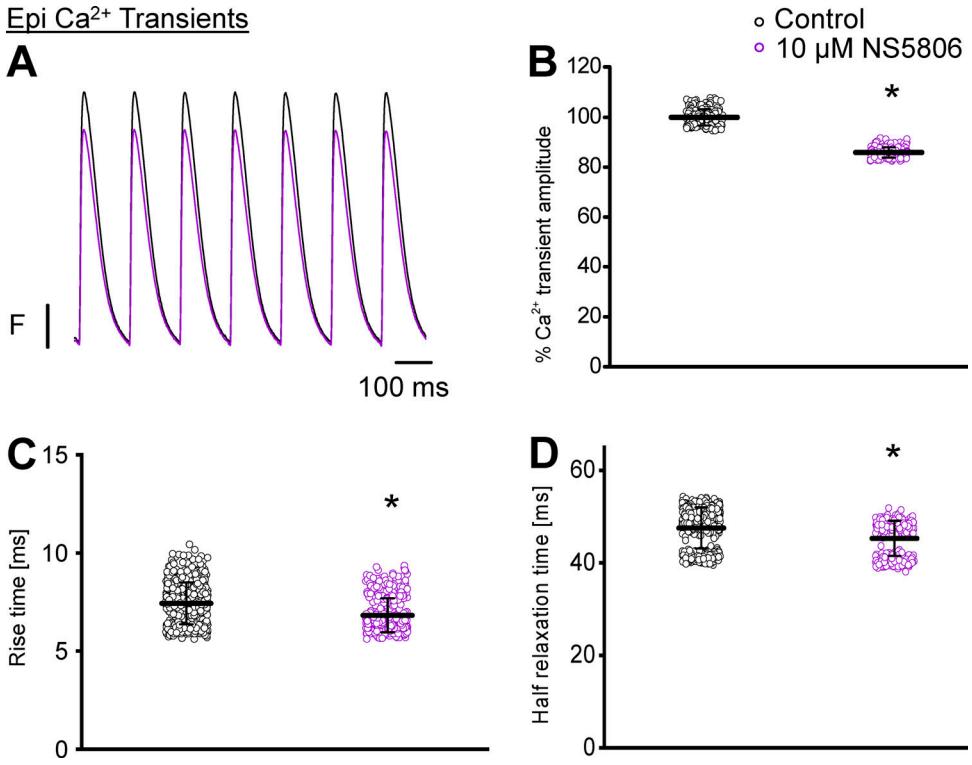

Figure 11. **NS5806 decreases the left ventricle developed pressure by decreasing the amplitude and the duration of Ca^{2+} transients. (A)** Effect of 10 µM NS5806 on the time course of epicardial Ca^{2+} transients. **(B)** The significant effect (*, P < 0.001) on the amplitude (100.1 ± 3.2%, 179 measurements for the control, black circles vs. 85.9 ± 2.1%, 180 measurements for NS5806, violet circles). **(C)** 10 µM NS5806 has a significant effect (*, P < 0.01) on the rise time of epicardial Ca^{2+} transients (7.42 ± 1.06 ms, 604 measurements for the control, black circles vs. 6.8 ± 0.8 ms, 480 measurements for NS5806, violet circles). **(D)** 10 µM NS5806 has a significant effect (*, P < 0.01) on the half relaxation time of epicardial Ca^{2+} transients (47.5 ± 4.4 ms, 594 measurements for the control, black circles vs. 45.1 ± 3.8 ms, 480 measurements for NS5806, violet circles). *n* = 4 hearts.

during phase 1 when the cardiac myocytes were paced at a pseudo-physiological heart rate. These experiments suggest that the effect depicted in the presence of 4-AP, in our experimental condition, is unlikely to be a consequence of Kv 1.5 block.

The effect of 4-AP on epicardial AP phase 1 is likely to impact on the ECG. As already shown by us, transmural ECG recordings in mouse hearts display a notable J wave (Kornyeyev et al., 2012). This J wave occurs because of the dissimilar rate of repolarization during phase 1 (Yan and Antzelevitch, 1996). Indeed, they reported that in dog ventricular wedge preparations, 4-AP decreases the amplitude of the J wave. Experiments presented in Fig. 4 show that in intact mouse hearts, 4-AP reduces the amplitude of the J wave (Fig. 4, C–E) and significantly widens its half duration (Fig. 4 D).

One possible explanation for the amplitude reduction in the J wave could be that 4-AP reduces the differences between the epicardial and endocardial rate of phase 1 repolarization. Fig. 5 shows not just a lag between endocardial and epicardial depolarization but a slower endocardial phase 1 repolarization, a result consistent with data from isolated mouse myocytes (Dilly et al., 2006). This difference can be explained by a decreased expression of Kv 4.3 at the endocardium (Brunet et al., 2004; Mattiazzi et al., 2015; Aguilar-Sanchez et al., 2017). Interestingly, the differences between endocardial and epicardial APD30 disappear when the hearts are perfused with 100 µM 4-AP (Fig. 5, C and F). Even more, no significant differences were observed at the APD90 level in both regions during 4-AP treatment (Fig. 5, D and G). In sum, 4-AP has a larger effect on the epicardium due to the higher expression of Kv. 4.3 in this layer, and the attenuation in the J wave by 4-AP occurs because of the decrease of the difference between epicardial versus endocardial phase 1 repolarization rates.

The fact that 4-AP has a larger effect on the epicardial than on the endocardial AP suggests that the contractility increase of the epicardial myocytes could be larger in the presence of the drug. This idea challenges the results published by Kondo et al. (2006) showing that 100 µM 4-AP has a larger effect on myocytes isolated from the left ventricular endocardium than on left ventricular epicardial cells. This discrepancy was ruled out in experiments presented in Fig. 6. As we expected, 100 µM 4-AP has a smaller effect on the amplitude of the endocardial Ca^{2+} transient. One possible explanation of the differences between Kondo et al. (2006) and our results is that their experiments were performed at room temperature under a bradycardic pacing rate (2 Hz). In contrast, our experiments were performed at 33°C and 7 Hz.

4-AP has a significant effect on both phase 1 repolarization rate and the transient change of myoplasmic Ca^{2+} during systole. The most likely scenario is that the slower rate of repolarization during phase 1 in the presence of 4-AP will drive an increase in

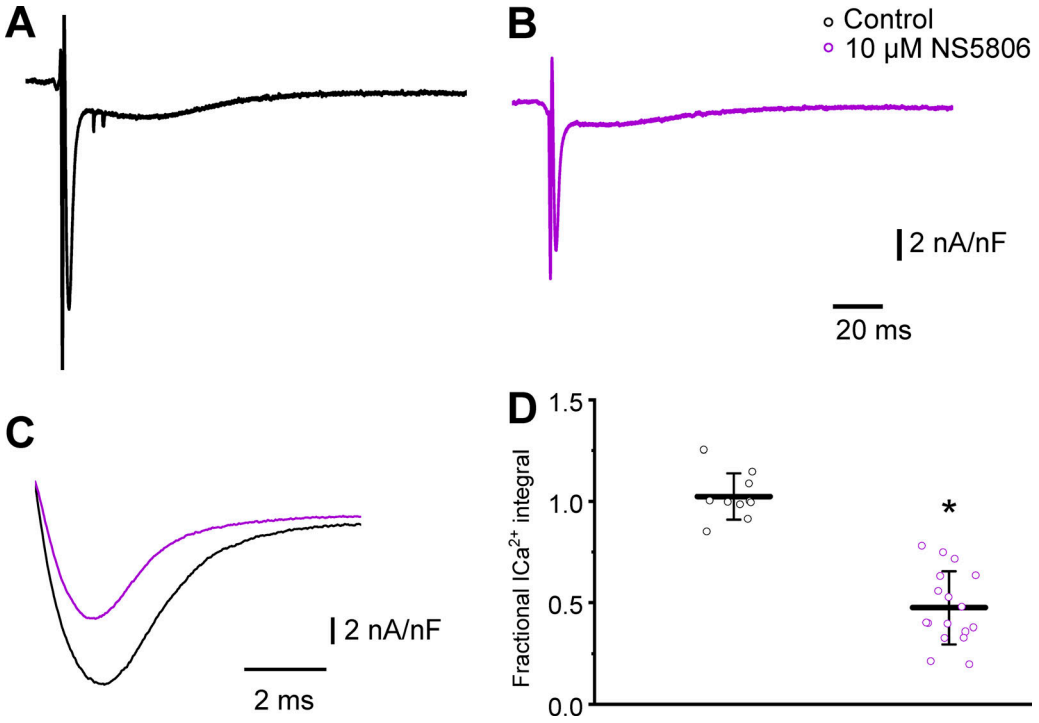

Figure 12. **NS5806 decreases the amplitude of Ca^{2+} transients by reducing Ca^{2+} influx through L-type Ca^{2+} channels. (A and B)** Effect of 10 μM NS5806 on the amplitude and kinetics of Ca^{2+}-mediated currents. **(C)** Comparison of the kinetics of the L-type Ca^{2+} current in the absence (black trace) and the presence (violet trace) of 10 μM NS5806. **(D)** Summarized significant effect (*, P < 0.001) of 10 μM NS5806. NS5806 reduces the amount of Ca^{2+} permeating (fractional integral of the Ca^{2+} current) into the myocytes (1.02 ± 0.11, 10 measurements the control, black circles vs. 0.47 ± 0.18, 17 measurements for NS5806, violet circles). *n* = 5 hearts.

the amplitude and duration of the L-type Ca^{2+} current. It has been shown that myocytes voltage clamped with AP waveforms having a slower phase 1 display a larger L-type Ca^{2+} current (Bányász et al., 2003). However, myocytes inhabiting the ventricular wall are highly electrically coupled. This induces an electrotonic coupling that can partially define the kinetics of the Ca^{2+} influx. We have recently developed the LPP technique (see Materials and methods) that allows the recording of Ca^{2+} currents when the myocytes from different layers are electrically and metabolically coupled. Fig. 7 shows that 4-AP significantly increases the amplitude and duration of the Ca^{2+} influx during phase 1. This result indicates that the increase in contractility observed during 4-AP treatment is due, at least in part, to an increased Ca^{2+} influx during systole.

I_{to} and L-type Ca^{2+} activation occur during AP phase 1. However, how much each of these currents participate in the kinetics of phase 1 repolarization has not been well established. Fig. 8 illustrates that in the absence of a Ca^{2+} influx through L-type channels, the repolarization during phase 1 is faster. This effect can be appreciated when the APD30 of a control AP is compared with an AP in which the Ca^{2+} current has been blocked. Moreover, if the same procedure is applied when I_{to} has been partially blocked with 100 μM 4-AP, the effect becomes dramatic. This result implies that the Ca^{2+} current is involved in defining the kinetics of phase 1. Furthermore, this also demonstrates that the 4-AP effect on APD30 is not only due to a blockage of I_{to} but also because I_{to} blockage influences the deactivation of the L-type Ca^{2+} current.

Interestingly, there is a spreading of the APD30 measurements as shown in Fig. 8 (B and C). The reason for this spreading is that the measurements are coming from different animals. It is important to remember that these are whole-heart experiments in which there are two main sources of variance. The first is that the hearts are not identical to each other; the second is that although we are measuring APs in the same region (the midregion of the left ventricle), it is impossible to perform the recordings in the same precise location between different hearts.

Phase 1 repolarization has a profound effect on epicardial and endocardial contractility. According to this idea, an increase in the phase 1 repolarization rate must induce a decrease in contractility. NS5806 has been used to increase I_{to} by slowing the inactivation rate of Kv 4.x. Fig. 9 (A–C) demonstrates that 10 μM NS5806 accelerates phase 1 and that this acceleration reduces the ventricular developed pressure (Fig. 10, A and B) and the amplitude and half duration of epicardial Ca^{2+} transients (Fig. 11, A–C). Interestingly, these effects on the Ca^{2+} transients affect the total duration of the AP (APD90) as shown in Fig. 9 C. The APD90 shortening is mostly produced by the lesser activation of the NCX in the forward mode, due to a decrease in the Ca^{2+} transient amplitude. Finally, the effect of NS5806 Ca^{2+} transients correlates with effect of NS5806 on the amplitude and the kinetics of the L-type Ca^{2+} current (Fig. 12, C and D). These results boost the idea that Kv.4.x channels regulate contractility. Moreover, although 4-AP can block other K^+ channels such as Kv 1.5, NS5806 only interacts with KChiP, a regulatory subunit that

interacts with Kv. 4.x channels and not with Kv 1.5 (Li et al., 2005).

Taken together, the results presented in this article demonstrate for the first time the role of I_{to} in defining cardiac contractility during the cardiac cycle of intact hearts. Furthermore, ventricular myocytes are electrically coupled in an environment having a step repolarization gradient. Thus, this step repolarization gradient can induce a graded contractility response across the ventricular wall. Finally, this suggests that the transmural differences in Ca^{2+} signaling are critical in defining the contractile properties of the free ventricular wall.

Acknowledgments

We thank Drs. Alicia Mattiazzi, Josefina Ramos-Franco, Julio Copello, Guillermo Perez, and Maria Zogbhi for their valuable discussions.

This study was supported by Fundação de Amparo à Pesquisa do Rio de Janeiro 219901 to M.M. López Alarcón; Coordenação de Aperfeiçoamento de Pessoal de Nível Superior Fellowship to A. Rodríguez de Yurre; a postdoctoral fellowship from Consejo Nacional de Investigaciones Científicas y Técnicas Argentina to J.I. Felice; and Proyectos de Investigación Científica y Tecnológica Raices 2524, University of California, Castle Facility UC-Castle-20095-442167, and National Institutes of Health 1R01GM132753-01 to A.L. Escobar.

The authors declare no competing financial interests.

Author contributions: A.L. Escobar conceived the project and designed the experiments. M.M. López Alarcón, A. Rodríguez de Yurre, J.I. Felice, E. Medei, and A.L. Escobar contributed to the data acquisition, analysis, and interpretation. A.L. Escobar and A. Rodríguez de Yurre wrote the manuscript, which was approved by all the authors. All the authors agree to be accountable for all aspects of the work, all those designated as authors qualify for authorship, and all those who qualify for authorship are listed.

Eduardo Ríos served as editor.

Submitted: 1 October 2018
Revised: 15 February 2019
Accepted: 15 March 2019

References

Aguilar-Sanchez, Y., D. Fainstein, R. Mejia-Alvarez, and A.L. Escobar. 2017. Local Field Fluorescence Microscopy: Imaging Cellular Signals in Intact Hearts. *J. Vis. Exp.* (121). https://doi.org/10.3791/55202

Almers, W., W.M. Roberts, and R.L. Ruff. 1984. Voltage clamp of rat and human skeletal muscle: measurements with an improved loose-patch technique. *J. Physiol.* 347:751–768. https://doi.org/10.1113/jphysiol.1984.sp015094

Bányász, T., L. Fülöp, J. Magyar, N. Szentandrássy, A. Varró, and P.P. Nánási. 2003. Endocardial versus epicardial differences in L-type calcium current in canine ventricular myocytes studied by action potential voltage clamp. *Cardiovasc. Res.* 58:66–75. https://doi.org/10.1016/S0008-6363(02)00853-2

Bouchard, R.A., R.B. Clark, and W.R. Giles. 1995. Effects of action potential duration on excitation-contraction coupling in rat ventricular myocytes. Action potential voltage-clamp measurements. *Circ. Res.* 76:790–801. https://doi.org/10.1161/01.RES.76.5.790

Brunet, S., F. Aimond, H. Li, W. Guo, J. Eldstrom, D. Fedida, K.A. Yamada, and J.M. Nerbonne. 2004. Heterogeneous expression of repolarizing, voltage-gated K+ currents in adult mouse ventricles. *J. Physiol.* 559:103–120. https://doi.org/10.1113/jphysiol.2004.063347

Cooper, P.J., C. Soeller, and M.B. Cannell. 2010. Excitation-contraction coupling in human heart failure examined by action potential clamp in rat cardiac myocytes. *J. Mol. Cell. Cardiol.* 49:911–917. https://doi.org/10.1016/j.yjmcc.2010.04.012

Cordeiro, J.M., L. Greene, C. Heilmann, D. Antzelevitch, and C. Antzelevitch. 2004. Transmural heterogeneity of calcium activity and mechanical function in the canine left ventricle. *Am. J. Physiol. Heart Circ. Physiol.* 286:H1471–H1479. https://doi.org/10.1152/ajpheart.00748.2003

Dilly, K.W., C.F. Rossow, V.S. Votaw, J.S. Meabon, J.L. Cabarrus, and L.F. Santana. 2006. Mechanisms underlying variations in excitation-contraction coupling across the mouse left ventricular free wall. *J. Physiol.* 572:227–241. https://doi.org/10.1113/jphysiol.2005.102020

Dong, M., X. Sun, A.A. Prinz, and H.-S. Wang. 2006. Effect of simulated $I_{(to)}$ on guinea pig and canine ventricular action potential morphology. *Am. J. Physiol. Heart Circ. Physiol.* 291:H631–H637. https://doi.org/10.1152/ajpheart.00084.2006

Escobar, A.L., P. Velez, A.M. Kim, F. Cifuentes, M. Fill, and J.L. Vergara. 1997. Kinetic properties of DM-nitrophen and calcium indicators: rapid transient response to flash photolysis. *Pflugers Arch.* 434:615–631. https://doi.org/10.1007/s004240050444

Escobar, A.L., C.G. Perez, M.E. Reyes, S.G. Lucero, D. Kornyeyev, R. Mejía-Alvarez, and J. Ramos-Franco. 2012. Role of inositol 1,4,5-trisphosphate in the regulation of ventricular Ca(2+) signaling in intact mouse heart. *J. Mol. Cell. Cardiol.* 53:768–779. https://doi.org/10.1016/j.yjmcc.2012.08.019

Ferreiro, M., A.D. Petrosky, and A.L. Escobar. 2012. Intracellular Ca^{2+} release underlies the development of phase 2 in mouse ventricular action potentials. *Am. J. Physiol. Heart Circ. Physiol.* 302:H1160–H1172. https://doi.org/10.1152/ajpheart.00524.2011

Fiset, C., R.B. Clark, T.S. Larsen, and W.R. Giles. 1997. A rapidly activating sustained K+ current modulates repolarization and excitation-contraction coupling in adult mouse ventricle. *J. Physiol.* 504:557–563. https://doi.org/10.1111/j.1469-7793.1997.557bd.x

Gómez, A.M., J.P. Benitah, D. Henzel, A. Vinet, P. Lorente, and C. Delgado. 1997. Modulation of electrical heterogeneity by compensated hypertrophy in rat left ventricle. *Am. J. Physiol.* 272:H1078–H1086. https://doi.org/10.1152/ajpheart.1997.272.3.H1078

Gonzalez, W.G., K. Pham, and J. Miksovska. 2014. Modulation of the voltage-gated potassium channel (Kv4.3) and the auxiliary protein (KChIP3) interactions by the current activator NS5806. *J. Biol. Chem.* 289:32201–32213. https://doi.org/10.1074/jbc.M114.577528

Guo, W., H. Xu, B. London, and J.M. Nerbonne. 1999. Molecular basis of transient outward K+ current diversity in mouse ventricular myocytes. *J. Physiol.* 521:587–599. https://doi.org/10.1111/j.1469-7793.1999.00587.x

Gurney, A.M., J.M. Nerbonne, and H.A. Lester. 1985. Photoinduced removal of nifedipine reveals mechanisms of calcium antagonist action on single heart cells. *J. Gen. Physiol.* 86:353–379. https://doi.org/10.1085/jgp.86.3.353

Huo, R., Y. Sheng, W.-T. Guo, and D.-L. Dong. 2014. The potential role of Kv4.3 K^+ channel in heart hypertrophy. *Channels (Austin).* 8:203–209. https://doi.org/10.4161/chan.28972

Knollmann, B.C., A.N. Katchman, and M.R. Franz. 2001. Monophasic action potential recordings from intact mouse heart: validation, regional heterogeneity, and relation to refractoriness. *J. Cardiovasc. Electrophysiol.* 12:1286–1294. https://doi.org/10.1046/j.1540-8167.2001.01286.x

Kondo, R.P., D.A. Dederko, C. Teutsch, J. Chrast, D. Catalucci, K.R. Chien, and W.R. Giles. 2006. Comparison of contraction and calcium handling between right and left ventricular myocytes from adult mouse heart: a role for repolarization waveform. *J. Physiol.* 571:131–146. https://doi.org/10.1113/jphysiol.2005.101428

Kornyeyev, D., M. Reyes, and A.L. Escobar. 2010. Luminal $Ca^{(2+)}$ content regulates intracellular $Ca^{(2+)}$ release in subepicardial myocytes of intact beating mouse hearts: effect of exogenous buffers. *Am. J. Physiol. Heart Circ. Physiol.* 298:H2138–H2153. https://doi.org/10.1152/ajpheart.00885.2009

Kornyeyev, D., A.D. Petrosky, B. Zepeda, M. Ferreiro, B. Knollmann, and A.L. Escobar. 2012. Calsequestrin 2 deletion shortens the refractoriness of Ca^{2+} release and reduces rate-dependent Ca^{2+}-alternans in intact mouse hearts. *J. Mol. Cell. Cardiol.* 52:21–31. https://doi.org/10.1016/j.yjmcc.2011.09.020

Li, H., W. Guo, H. Xu, R. Hood, A.T. Benedict, and J.M. Nerbonne. 2001. Functional expression of a GFP-tagged Kv1.5 alpha-subunit in mouse ventricle. *Am. J. Physiol. Heart Circ. Physiol.* 281:H1955–H1967. https://doi.org/10.1152/ajpheart.2001.281.5.H1955

Li, H., W. Guo, R.L. Mellor, and J.M. Nerbonne. 2005. KChIP2 modulates the cell surface expression of Kv 1.5-encoded K(+) channels. *J. Mol. Cell. Cardiol.* 39:121–132. https://doi.org/10.1016/j.yjmcc.2005.03.013

Mattiazzi, A., M. Argenziano, Y. Aguilar-Sanchez, G. Mazzocchi, and A.L. Escobar. 2015. Ca2+ Sparks and Ca2+ waves are the subcellular events underlying Ca2+ overload during ischemia and reperfusion in perfused intact hearts. *J. Mol. Cell. Cardiol.* 79:69–78. https://doi.org/10.1016/j.yjmcc.2014.10.011

Mejía-Alvarez, R., C. Manno, C.A. Villalba-Galea, L. del Valle Fernández, R.R. Costa, M. Fill, T. Gharbi, and A.L. Escobar. 2003. Pulsed local-field fluorescence microscopy: a new approach for measuring cellular signals in the beating heart. *Pflugers Arch.* 445:747–758. https://doi.org/10.1007/s00424-002-0963-1

Morad, M., Y.E. Goldman, and D.R. Trentham. 1983. Rapid photochemical inactivation of Ca2+-antagonists shows that Ca2+ entry directly activates contraction in frog heart. *Nature.* 304:635–638. https://doi.org/10.1038/304635a0

Nerbonne, J.M., and R.S. Kass. 2005. Molecular physiology of cardiac repolarization. *Physiol. Rev.* 85:1205–1253. https://doi.org/10.1152/physrev.00002.2005

Ramos-Franco, J., Y. Aguilar-Sanchez, and A.L. Escobar. 2016. Intact Heart Loose Patch Photolysis Reveals Ionic Current Kinetics During Ventricular Action Potentials. *Circ. Res.* 118:203–215. https://doi.org/10.1161/CIRCRESAHA.115.307399

Roberts, W.M., and W. Almers. 1984. An improved loose patch voltage clamp method using concentric pipettes. *Pflugers Arch.* 402:190–196. https://doi.org/10.1007/BF00583334

Rossow, C.F., K.W. Dilly, and L.F. Santana. 2006. Differential calcineurin/NFATc3 activity contributes to the Ito transmural gradient in the mouse heart. *Circ. Res.* 98:1306–1313. https://doi.org/10.1161/01.RES.0000222028.92993.10

Rossow, C.F., K.W. Dilly, C. Yuan, M. Nieves-Cintrón, J.L. Cabarrus, and L.F. Santana. 2009. NFATc3-dependent loss of I(to) gradient across the left ventricular wall during chronic β adrenergic stimulation. *J. Mol. Cell. Cardiol.* 46:249–256. https://doi.org/10.1016/j.yjmcc.2008.10.016

Sah, R., R.J. Ramirez, and P.H. Backx. 2002. Modulation of Ca(2+) release in cardiac myocytes by changes in repolarization rate: role of phase-1 action potential repolarization in excitation-contraction coupling. *Circ. Res.* 90:165–173. https://doi.org/10.1161/hh0202.103315

Sah, R., R.J. Ramirez, G.Y. Oudit, D. Gidrewicz, M.G. Trivieri, C. Zobel, and P.H. Backx. 2003. Regulation of cardiac excitation-contraction coupling by action potential repolarization: role of the transient outward potassium current (I_{to}). *J. Physiol.* 546:5–18. https://doi.org/10.1113/jphysiol.2002.026468

Said, M., R. Becerra, J. Palomeque, G. Rinaldi, M.A. Kaetzel, P.L. Diaz-Sylvester, J.A. Copello, J.R. Dedman, C. Mundiña-Weilenmann, L. Vittone, and A. Mattiazzi. 2008. Increased intracellular Ca2+ and SR Ca2+ load contribute to arrhythmias after acidosis in rat heart. Role of Ca2+/calmodulin-dependent protein kinase II. *Am. J. Physiol. Heart Circ. Physiol.* 295:H1669–H1683. https://doi.org/10.1152/ajpheart.00010.2008

Sanchez, J.A., and J. Vergara. 1994. Modulation of Ca2+ transients by photorelease of caged nucleotides in frog skeletal muscle fibers. *Am. J. Physiol.* 266:C1291–C1300. https://doi.org/10.1152/ajpcell.1994.266.5.C1291

Teutsch, C., R.P. Kondo, D.A. Dederko, J. Chrast, K.R. Chien, and W.R. Giles. 2007. Spatial distributions of Kv4 channels and KChip2 isoforms in the murine heart based on laser capture microdissection. *Cardiovasc. Res.* 73:739–749. https://doi.org/10.1016/j.cardiores.2006.11.034

Valverde, C.A., D. Kornyeyev, M. Ferreiro, A.D. Petrosky, A. Mattiazzi, and A.L. Escobar. 2010. Transient Ca2+ depletion of the sarcoplasmic reticulum at the onset of reperfusion. *Cardiovasc. Res.* 85:671–680. https://doi.org/10.1093/cvr/cvp371

Volk, T., T.H. Nguyen, J.H. Schultz, and H. Ehmke. 1999. Relationship between transient outward K+ current and Ca2+ influx in rat cardiac myocytes of endo- and epicardial origin. *J. Physiol.* 519:841–850. https://doi.org/10.1111/j.1469-7793.1999.0841n.x

Yan, G.X., and C. Antzelevitch. 1996. Cellular basis for the electrocardiographic J wave. *Circulation.* 93:372–379. https://doi.org/10.1161/01.CIR.93.2.372

Zimmer, H.-G. 1998. The Isolated Perfused Heart and Its Pioneers. *News Physiol. Sci.* 13:203–210.

Zygmunt, A.C., D.C. Robitelle, and G.T. Eddlestone. 1997. Ito1 dictates behavior of ICl(Ca) during early repolarization of canine ventricle. *Am. J. Physiol.* 273:H1096–H1106. https://doi.org/10.1152/ajpheart.1997.273.3.H1096